Proceedings of the IASS 2024 Symposium
Redefining the Art of Structural Design
August 26-30, 2024, Zurich Switzerland
Philippe Block, Giulia Boller, Catherine DeWolf,
Jacqueline Pauli, Walter Kaufmann (eds.)

Rethinking Naturally Shaped flexible grid structures combining bending and twisting

Fereshteh KHOJASTEHMEHR*, Günther H. FILZ

*Universität Innsbruck, Faculty of Architecture, LSU Lightweight Structures Unit
Technikerstrasse 21c, 6020 Innsbruck, Austria
Fereshteh.Khojastehmehr@uibk.ac.at

Abstract

Flexible grid structures are considered efficient structures due to their form, structural performance, and low material consumption. For many years, the search for optimal structural forms of elastic grids has been mainly based on repetitive patterns with changing boundary conditions and cross-section of the grid by multi-layer lattices. In our previous paper, we have shown the potential of applying twist in elastic structures to increase the design freedom to achieve self-organizing forms. Unlike the common grid structures that usually have a constant surface thickness, the depth of our structure varies by rotating the profile of the strip along its longitudinal axis. Twist allows for a smooth transition from one pattern type such as geodesic to another such as asymptotic with a 90° rotation of the flexible strip profile. In this paper, we compare a simple grid with three different patterns - asymptotic, geodesic, and their combination by twisting the strip profile - from architectural aspects such as density, view, shadow, pattern, and structural aspects, including the deflection of the structural form. Considering the material behavior and introducing bending and twist as the actuators of the self-forming process, the resulting grid structures are naturally formed, provide highly variant options for design and in some cases show structurally well performing results. This approach promotes the use of elastic grid structures making them viable options in multi-objective architectural design.

Keywords: Spatial structures, elastic gridshell, twist, geometrical pattern, Gaussian curvature, architectural geometry, structural morphology, multi-objective design, timber and bio-based spatial structures.

1. Introduction to flexible grid structures

Grid structures, similar to shells, are efficient lightweight structures due to lowering material consumption. Elastic gridshells minimize or eliminate the necessity for expenses and energy in fabricating curved elements, as they can be flexibly bent to create curvilinear shapes [1, 2]. The transportation of the elements to the construction site is also streamlined, as they are manufactured as straight, linear or planar elements and can be packed into a smaller volume compared to curvilinear elements produced using CNC milling devices. As the strips or grid elements are typically cut from boards or sheet material, the amount of material waste is also reduced compared to other subtractive fabrication techniques.

The initial constructed instance of flexible grid structures was erected in 1896, employing steel by Shukhov [1, 3]. Modern timber gridshells were followed in 1960s with examples such as Essen Pavilion in 1962 and the German Pavilion in 1967 [4, 5]. Elastic gridshells are commonly designed using two methods: a pattern-first approach, which begins with the grid or pattern brought into defined boundary conditions; and a shape-first approach, where a predefined shape or surface is considered, and the pattern is subsequently applied to it [6, 7]. Most of these flexible grid structures have a dome-like form with geometrical usually repetitive patterns [8–10]. In elastic gridshells the two pattern types of geodesic [11–13] and asymptotic [14, 15] are most commonly used. Different definitions for geodesic curves include "the straightest curves", "the shortest curves", and the "less bent curves" on a surface [16]. Geodesic curves and strips are developable surfaces meaning that they can be flattened [17]. Asymptotic line and strips can be also unrolled into flat straight linear elements [18]. Schling et al. [19] suggested and applied a hybrid pattern using a layer of geodesic and a layer of asymptotic. Further development is needed in researching the integration of these two pattern types, emphasizing their harmonious combination instead of treating them as separate layers.

Applying twist in the profile has shown effective results in changing the surface curvature, surface depth, and smooth transitioning between the pattern types of geodesic and asymptotic [20]. Besides formal opportunities, shifting between the profile directions also responds to the structural performance. Usually in structural optimization, lowering the structure's weight, while ensuring stability and strength against buckling are considered as main objectives [21]. This can be accomplished through methods such as profile modification, also known as shape optimization, aimed at reducing material consumption and achieving higher structural efficiency. Reducing the weight of the structure and material consumption is a beneficial aspect of these methods. However, removing material from a mass, such as a timber beam, results in waste. Utilizing the flexibility of the material and employing elastic twisting in the weak axis of the profile, we can transition between different cross-sections without cutting to shape, which usually generates additional waste.

We propose combined geodesic-asymptotic patterns within the same grid structure, and compare and evaluate the resulting grid structure with the two common pattern types: geodesic and asymptotic. While in geodesic pattern the profile is tangential to the surface and in asymptotic pattern the profile is perpendicular to the surface, in a combined geodesic-asymptotic pattern the profile twists in the longitudinal axis transitioning from one to the other pattern type. This results in change in characteristics including change in the surface depth, surface curvature, as well as structural performance. For the simulation and structural analysis, a Birch-Conifer Combi Plywood with a thickness of 6.5 mm and a density of 620 kg/m³, as specified by the manufacturer [22] was assumed as material.

In a first step, we start with patterns instead of a predefined surface. We simulate the structural form for each of these three pattern types and observe the results. The simulation utilizes mesh and rod relaxation using Kangaroo Physics [23], a plugin for Grasshopper3D and Rhino3D. Subsequently, we compare the generated forms from different aspects of architecture such as surface curvature, view, shadow, transparency and density, and from a structural perspective including deflections using Karamba3D [24].

In a second step, the geodesic, asymptotic, and combined geodesic-asymptotic pattern types are applied on a predefined surface to follow the surface curvature. We compare and evaluate the compatibility of these three pattern types with different parts of the predefined surface and their impact on architectural and structural aspects. The results of this research enhance our comprehension of the impact of pattern types, especially the influence of profile twist, on the architectural and structural aspects of resulting forms, introducing them as viable options for multi-objective design.

2. Twist

Twisting involves rotating or distorting one object around another [25]. Torque is additionally described as a force leading to rotation or torsion [26, 27]. Elastic twist is getting importance in the recent research works [20, 28, 29]. Applying twist on the longitudinal axis of the profile changes the curvature of the strip and the resulting patched surface from the elements' mesh vertices [20]. Shifting between different profile directions by applying twist on the longitudinal axis of the profile also results in a change of the transparency, density, surface depth, and structural performance. Twisting the longitudinal profiles of elements in a grid induces changes in curvature across the crossing elements. We explore the elastica curve of the crossing elements to follow the curvature change applied to them while considering the minimum bending radius of the material.

Figure 1 shows an example of generating a self-organized crossing strip on four twisted longitudinal elements. In the first step, the longitudinal elements are 180° twisted, in two opposing directions using mesh relaxation. In the second step, the crossing strip's path is placed to find the connecting points to the longitudinal strips. The third step is dedicated to finding the elastica curve of the crossing strip formed by rod relaxation. The gray circles in Figure 1 show the curvature on evaluated points of the crossing curve. The radius of these circles should not pass the limits of the material's minimum bending radius. In the fourth step, the respective profile follows the individual paths as illustrated in the steps of Figure 1.

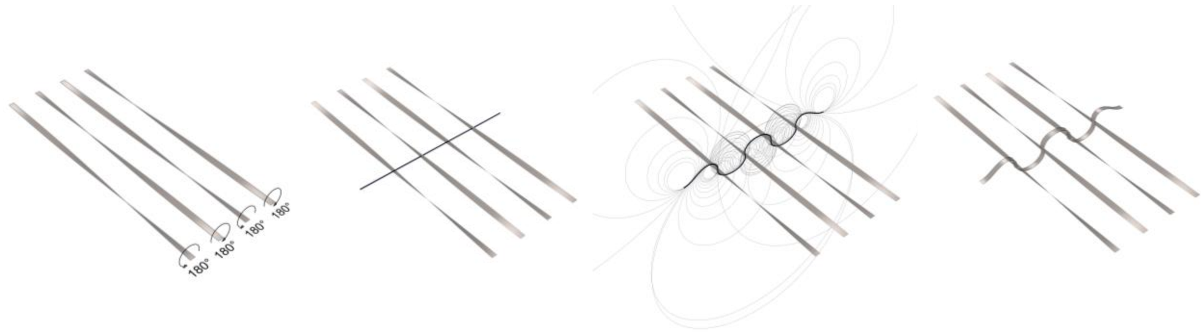

Step 1 Step 2 Step 3 Step 4

Figure 1: The generation of a self-organized crossing strip on the longitudinal twisted strips. From Left to right: 180° twist in the longitudinal elements, finding the path of the crossing strip, exploring the elastica curve from the initial crossing path, and applying the profile on the elastica curve.

The generation of crossing strips is self-organized, as the material dictates the form of the strip, and we solely define the crossing path. These curvilinear forms result from the degree and direction of twist applied to the longitudinal profiles.

Considering the same process in a flat state, we generate an exemplifying grid of strips with the width of 6 cm, a thickness of 6.5 mm and two lengths of 3 m and 1.8 m, with an asymptotic (Figure 2-left) and a geodesic pattern (Figure 2-center). Figure 2-right illustrates a twisted pattern generated by rotating the longitudinal elements to create a strong axis of the profile in the center. It is worth mentioning that due to the twist in the material, curvature is imparted to the elements, necessitating the addition of material length to prevent breakage. For example, in the same grid of Figure 2, with the same width and thickness of the strips, the length addition needed for the twisted pattern results in 0.327 m^2 added material.

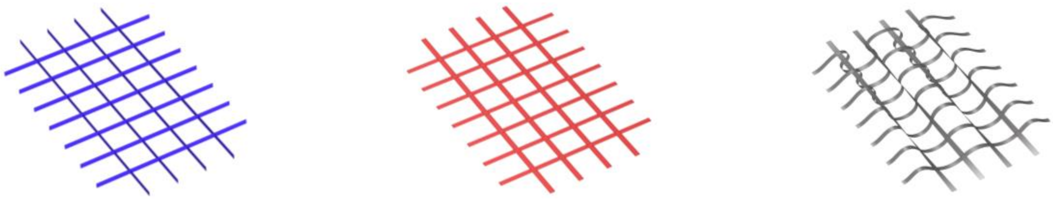

used material = 1.419 m^2 used material = 1.419 m^2 used material = 1.746 m^2

Figure 2: An asymptotic (left), a geodesic (center), and a twisted (right) pattern.

To gain insight into the curvature change of the generated pattern resulting from the twisted elements, we create a patch surface from the mesh vertices. It is important to mention that these surfaces are generated after the generation of the strip meshes and are indicators of the imaginary curved forms. We define two parameters of surface deformation: surface deformation (dv), representing the distance between the highest and lowest points of the mesh, and mean Gaussian curvature (MGC), the average Gaussian curvature of the surface, to compare the generated surfaces. Figure 3 shows the surface deformation and the mean Gaussian curvature of the geodesic, asymptotic, and the twisted pattern. While the surface deformation and Gaussian curvature remain constant in a geodesic and an asymptotic pattern, these values vary across the surface for a twisted pattern.

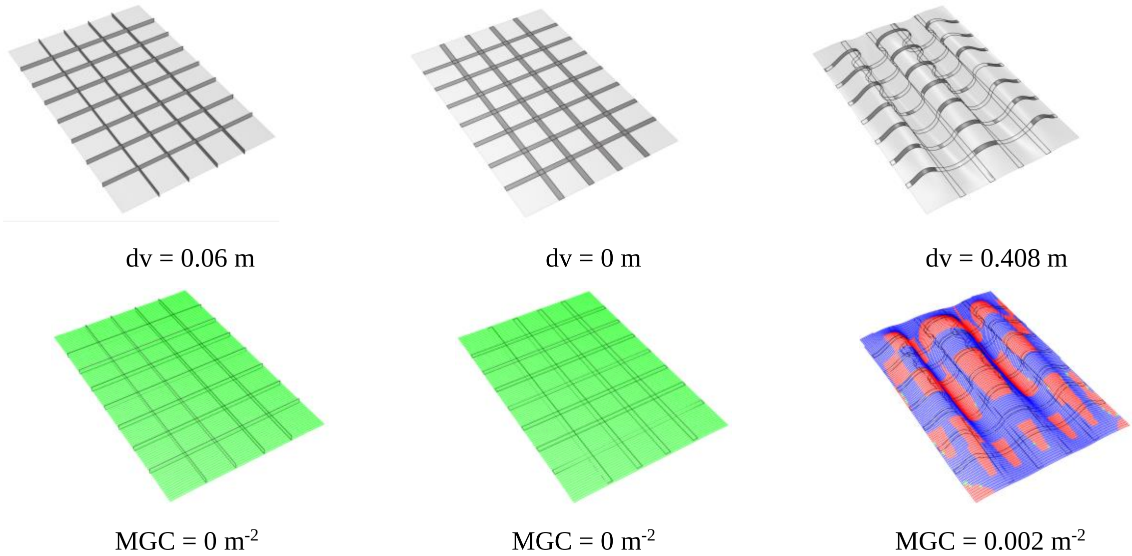

Figure 3: The comparison of the surface curvature. From left to right: an asymptotic, a geodesic, and a twisted pattern. Green, red, and blue represent zero, positive, and negative Gaussian curvature regions respectively.

In addition to the overall shape of the generated surface, aspects including transparency and shadow also change for a twisted pattern. Density is measured by the number of elements in a square meters and transparency is the amount of material used in the same area [8]. While the density is the same in the three pattern types because of keeping the same grid, the transparency differs based on the profile direction. The asymptotic pattern has the highest transparency while geodesics has the least. In the twisted pattern, the transparency varies across the surface due to the twist in the profile's longitudinal axis and the transition between different profile directions. The transparency and the generated shadow of these pattern are shown in Figure 4.

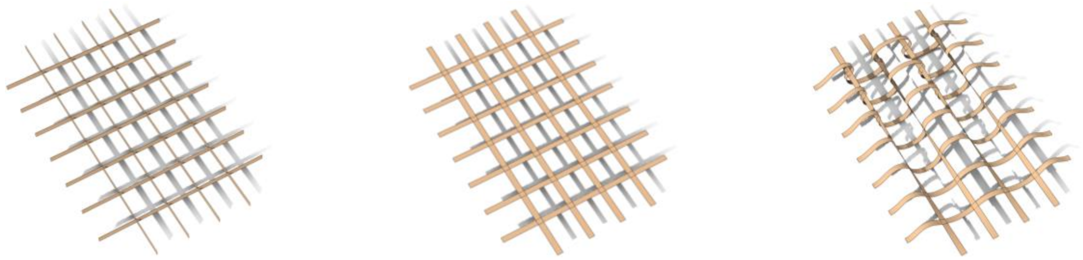

Figure 4: From left to right: an asymptotic, a geodesic, and a twisted pattern and their corresponding shadows.

In the following section, we investigate the geodesic, asymptotic, and combined geodesic-asymptotic patterns on a predefined surface, along with their corresponding architectural and structural aspects.

3. Combined geodesic-asymptotic grid structures

Due to the characteristics of geodesic and asymptotic patterns, they follow a path that suits their geometrical requirements. For example, the asymptotic curves can be generated in the anticlastic and zero Gaussian curvature surface areas and in practice they cannot be extended to the synclastic regions [18, 30]. For example, as shown in Figure 5, on a surface with a combination of synclastic (positive Gaussian curvature), anticlastic (negative Gaussian curvature), and zero Gaussian curvature, the asymptotic pattern can be generated in the anticlastic region.

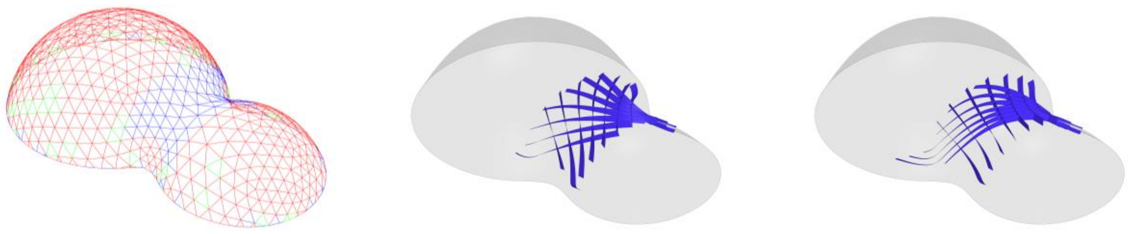

Figure 5: A predefined surface (left) with negative (blue), positive (red), and zero (green) Gaussian curvature regions and two asymptotic patterns on the anticlastic regions of the predefined surface (center and right).

Geodesic patterns, unlike asymptotic (with strips perpendicular to surface), can be generated on any type of surface. We can define the start and end point of the geodesic curves. They however, follow a certain path considering the curvature of the surface. Two examples of geodesic patterns are shown on the same surface in Figure 6. As the paths of the strips show, the concentration on the anticlastic region is higher due to the higher curvature of the surface in this area.

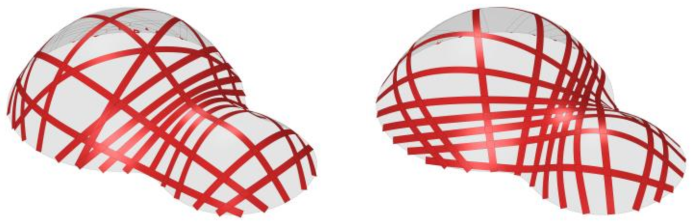

Figure 6: Two examples of geodesic patterns on a predefined surface.

Since generating an asymptotic pattern alone on this surface is not feasible, our comparison is limited to a geodesic pattern and a combined geodesic-asymptotic pattern. Figure 7 shows the transparency change in the combined geodesic-asymptotic patterns as a comparison to the geodesic ones. The shadows change by the combined geodesic-asymptotic patterns also contribute to their aesthetics as an architectural feature. The process of generating the combined geodesic-asymptotic pattern is explained in another example on an anticlastic surface.

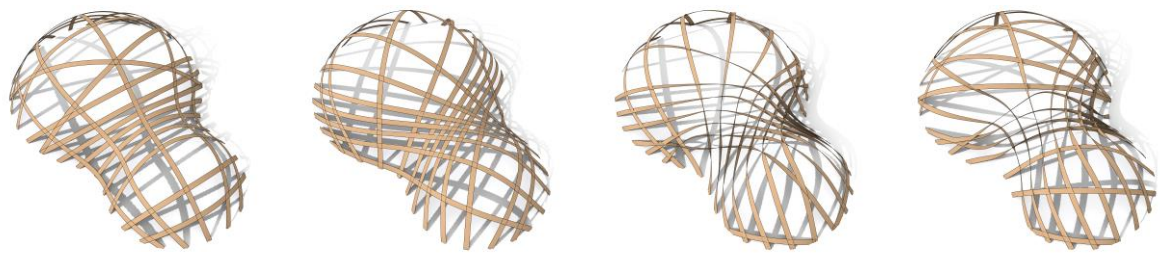

geodesic 1 | geodesic 2 | combined 1 | combined 2

Figure 7: Two geodesic and two combined patterns and their corresponding shadows.

If our aim is solely to maintain tangential and perpendicular profile directions, rather than adhering strictly to the geodesic and asymptotic patterns, we can generate similar grids by projecting them onto the surface. It is important to mention that in this method, the generated geometrical elements do not follow the geodesic and asymptotic path. The unrolled version of these strips may also be non-straight or even possible to planarize. Figure 8 illustrates one strip positioned as the same grid element in three profile directions: perpendicular (Figure 8-left), tangential (Figure 8-center), and twisted profiles (Figure 8-right), along with their unrolled strip surfaces revealing non-straight outlines. This curvilinear outline usually necessitates material waste due to the creation of cut-offs, as depicted in gray color at the bottom of Figure 8. This is in contrast to the geodesic and asymptotic paths that create straight planar outlines.

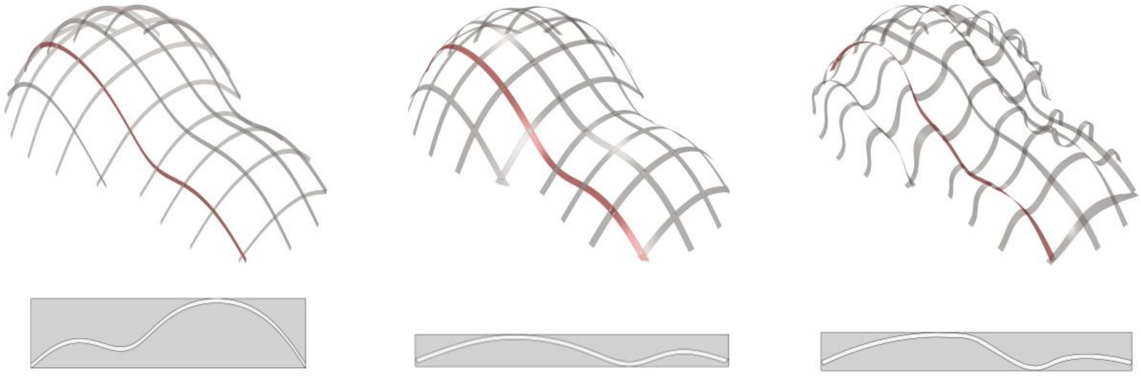

Figure 8: A perpendicular (left), a tangential (center), and a twisted (right) profile patterns and their unrolled surface of one strip.

We consider a simple anticlastic surface to generate geodesic, asymptotic, and combined geodesic-asymptotic patterns that can be unrolled into a straight planar state. This allows for further architectural and structural comparison of these three pattern types. This surface with an overall size of 3m x 2m x 1m, as shown in Figure 9.

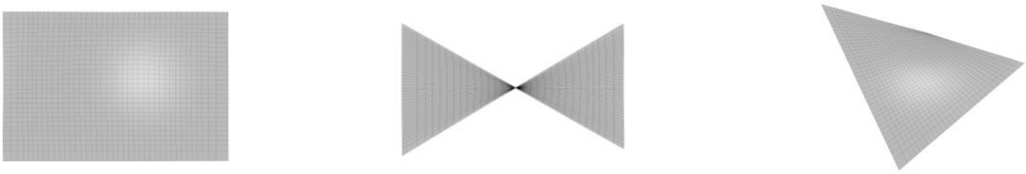

Figure 9: The predefined anticlastic surface in a top view (left), a side view (center), and a perspective view (right).

A grid of strips with a width of 10 cm, a thickness of 6.5 mm, and the three pattern types of a geodesic, an asymptotic, and a combination by applying twist are applied on this predefined surface. The pattern generation for the combined geodesic-asymptotic starts from the asymptotic curves and uses its endpoints as the start of the geodesic paths. An example of a combined geodesic-asymptotic pattern is shown in Figure 10. In this example, the surface is subdivided into two equal-sized regions of asymptotic and geodesic and the transition in between is simulated informed by the material properties.

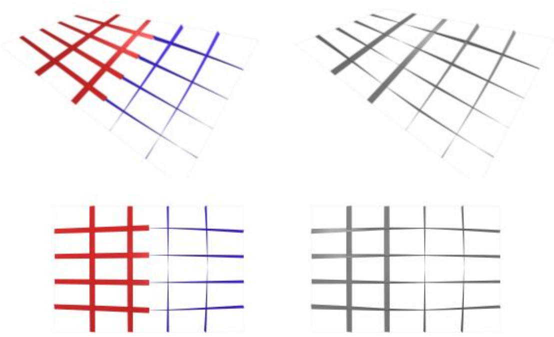

Figure 10: The process of generating a combined geodesic-asymptotic pattern. Left-before merging the patterns, right-after merging the two patterns into one.

We generate two combined geodesic-asymptotic patterns with almost the same area, compared to the geodesic and asymptotic patterns (Figure 11). This allows for structural performance comparison between the pattern types calculation, which in here is implemented based on the structure's self-weight. Supports are placed at the endpoints of the strips, and joints connecting the crossing elements are defined in the analysis. To show the potential of design control for the combined geodesic-asymptotic patterns, we consider a rule where 1/4 of the surface is asymptotic to have high transparency and the other regions are geodesic or transition regions. Similar to the process outlined in Figure 10, the combined patterns in Figure 11 are generated starting from the asymptotic pattern within the defined region, on the bottom-right corner of the surface as shown in the top view. Geodesic curves are subsequently added, originating from the endpoints of the asymptotic curves and ending at the edges of the boundary rectangle. In the first combined geodesic-asymptotic pattern, the geodesic curves are identical to those in both the geodesic and asymptotic patterns, while in the second combined geodesic-asymptotic pattern, the paths are altered.

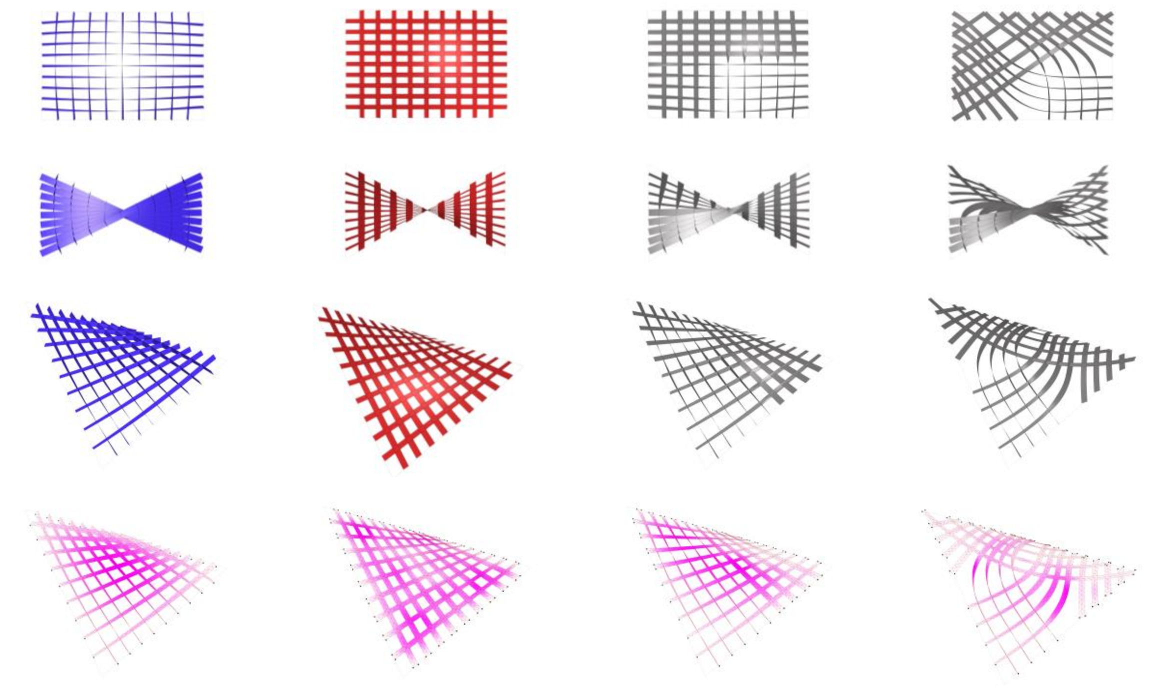

used material = 5.387 m²	used material = 5.387 m²	used material = 5.361 m²	used material = 5.15 m²
displacement = 4 mm	displacement = 2 mm	displacement = 6 mm	displacement = 3 mm

Figure 11: From left to right: an asymptotic, a geodesic, and two combined geodesic-asymptotic patterns. From top to bottom: the top view, side view, perspective view, and displacement

The structural performance of the combined geodesic-asymptotic patterns, compared to the geodesic and asymptotic patterns, yields similar results, although it may vary depending on the specific pattern. It's important to note that in displacement, the heatmap in each structure is based on its individual domain, making it difficult to compare the structures at first glance. As shown in Figure 11, the displacement of the combined geodesic-asymptotic pattern falls between that of a geodesic and an asymptotic pattern. The displacement heatmap shows that the largest displacement for geodesic and asymptotic patterns is mostly in the centric regions of the surface, while in the combined geodesic-asymptotic patterns this largest displacement region is shifted from the center to the transition regions where twist is applied to the profile. The combined geodesic-asymptotic pattern is designed not only to meet structural performance requirements but also to fulfill architectural objectives. As depicted in Figure 12, while the cross-section remains consistent in the geodesic pattern, the combined geodesic-asymptotic pattern allows for a smooth transition between asymptotic and geodesic pattern regions, resulting in greater changes in transparency, surface depth, and resulting shadow. This transition creates a dynamic pattern with varying levels of transparency across the surface, unlike the constant profile direction observed in asymptotic and geodesic surfaces.

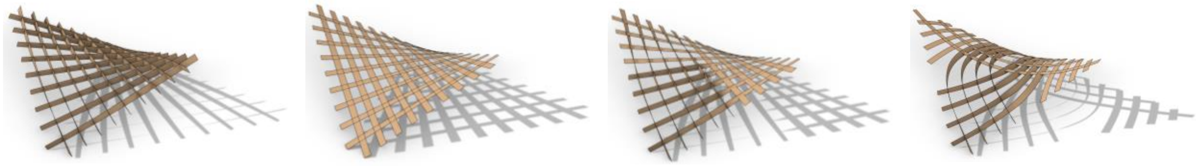

Figure 12: The transparency and shadows in from left to right an asymptotic, a geodesic, and two combined geodesic-asymptotic patterns.

To underscore the potential of the combined geodesic-asymptotic patterns, we present another example applying the geodesic, asymptotic, and combined geodesic-asymptotic patterns on the anticlastic surface depicted in Figure 13. This torus surface measures 5m x 2.5m x 2.5m overall.

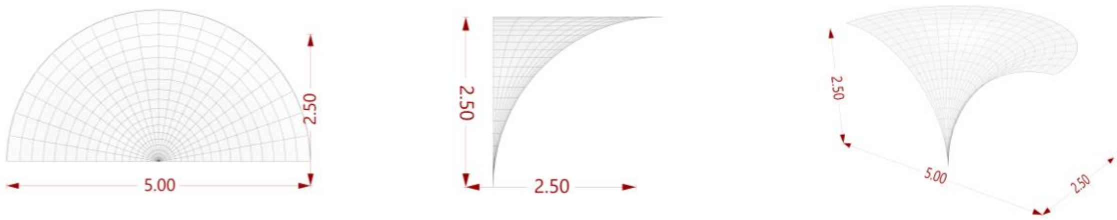

Figure 13: A predefined Torus surface in a top view (left), side view (center), and perspective view (right).

The structural analysis focuses on strips of flexible plywood with a thickness of 0.9cm and a width of 0.1m, with varying lengths determined by the patterns. Similar to the previous example, the loading consists solely of structure weight. To ensure a fair comparison, all three patterns use nearly the same amount of material. The patterns are depicted in Figure 13 (top), structural displacement in Figure 13 (center), and transparency and shadows in Figure 13 (bottom).

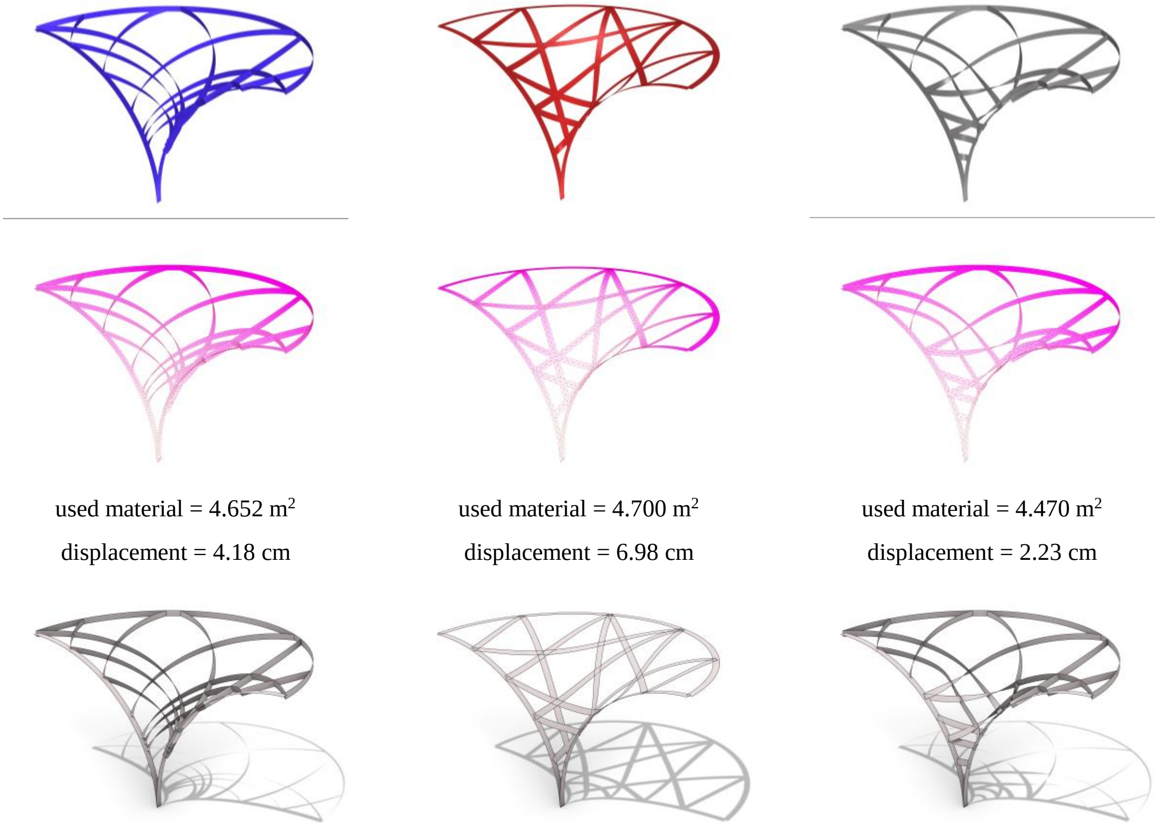

Figure 14: From left to right: an asymptotic, a geodesic, and a combined geodesic-asymptotic patterns. From top to bottom: patterns, displacements, and shadows.

The reduced displacement of the combined geodesic-asymptotic pattern, compared to the geodesic and asymptotic patterns in this example, demonstrates the effect of strategically transitioning between profile directions to geometrically respond to load transitions. Alongside their structural performance, the aesthetical features of these structures make them unique architectural elements. Figure 15 visualizes the application of the combined geodesic-asymptotic pattern as a canopy.

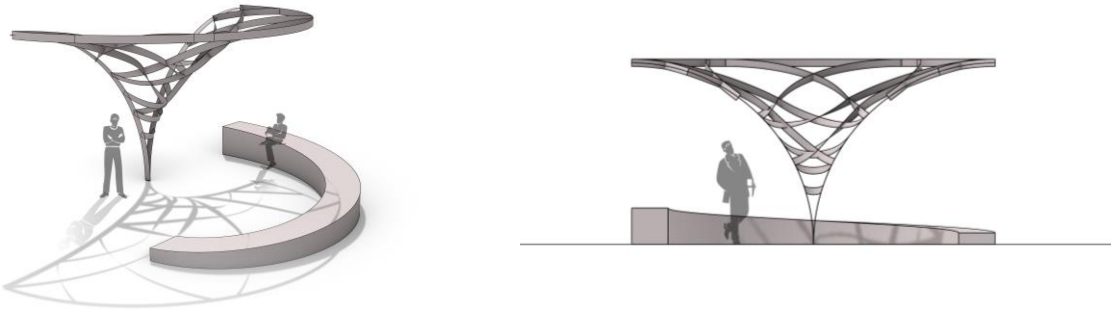

Figure 15: A combined geodesic-asymptotic pattern used as a canopy structure.

4. Results

Applying a twist to the profile of elements results in a change in surface curvature and structural performance. The twisted patterns are capable of creating curvilinear forms even from a simple flat grid of elements, resulting in a curvature deformation of up to 13% of the span.

Based on our experiments on an anticlastic surface with almost the same amount of material for different pattern types, the structural performance is within an acceptable range, considering the proportion of displacement to span. The torus surface example further demonstrates the potential of the combined geodesic-asymptotic patterns for canopy structures, achieving a 50% reduction in displacement compared to the asymptotic pattern and a one-third reduction compared to the geodesic pattern. These experiments validate the use of twist in grid structures. Besides acceptable structural performance, the transparency and shadow also vary across the surface in a combined geodesic-asymptotic pattern, contrasting with their consistent appearance in a geodesic or an asymptotic pattern.

5. Discussion and Conclusion

This paper presents a method for designing combined geodesic-asymptotic flexible grid structures. Introducing a twist on the longitudinal axis of the profiles allows for smooth transitioning between different pattern types of geodesic and asymptotic. As the asymptotic pattern is limited to specific curvature types, mostly anticlastic regions, we simulate and generate a geodesic, an asymptotic, and a combined geodesic-asymptotic pattern on an anticlastic surface. We simulate these three pattern types and compare the architectural features including density, transparency, shadow, and depth of the surface, and structural aspects including deflection. The simulation also takes into account the behavior of the material, with the curvature of the pattern being derived from it.

The variations in surface curvature, depth, transparency, and shadow, coupled with the structural performance of these structures, offer the potential to address multiple design objectives in architecture. This makes them viable options as alternatives for traditional elastic gridshells. The resulting form may exhibit varying architectural and structural qualities depending on the pattern and surface curvature.

In recent studies, it has been observed that curved shapes are often considered appealing. Users tend to regard spaces as beautiful if they exhibit curvilinear features and such spaces are also perceived as more pleasant, sociable, and conducive to creativity [31]. Other methods for integrating different cross-sections such as adding cuts and interlocking the profiles could be another method for transitioning between different pattern types which makes cut-offs and also due to our aim of flexibility and smooth transitioning are not considered. In our ongoing research, the design process explained in this paper is being incorporated into a larger, prototypical architectural project. We hypothesize that the new possible structural-architectural variants of the presented self-organized grid structures will inspire the further application of elastic grid shells and remind of their golden era, as can be seen in projects such as the Multihalle Mannheim.

Acknowledgements

This research was funded by the University of Innsbruck as an early-stage funding 2022.

References

[1] J. Lienhard, "Bending-Active Structures: Form-finding strategies using elastic deformation in static and kinetic systems and the structural potentials therein," PhD Dissertation, ITKE, University of Stuttgart, Stuttgart, Germany, 2014.
[2] E. L. Hernández, "Design and Optimisation of Elastic Gridshells," PhD thesis, Institut für Konstruktives Entwerfen und Tragwerkslehre, Universität der Künste Berlin, Berlin, Germany, 2015.
[3] International Database and Gallery of Structures, *Rotunda of the Panrussian Exposition.* [Online]. Available: https://structurae.net/en/structures/rotunda-of-the-panrussian-exposition (accessed: Apr. 2 2024).
[4] J. Chilton and G. Tang, *Timber gridshells: Architecture, structure and craft*. London, New York: Routledge, 2017.
[5] E. Happold and W. I. Liddell, "Timber lattice roof for the Mannheim Bundesgartenschau," *Structural Engineer*, vol. 53, no. 3, 1975.
[6] M. H. Saleh Tabari, F. Khojastehmehr, and G. H. Filz, "Parametric thinking for decision-making in elastic gridshell design," in *Proceedings of the IASS Annual Symposium 2022*, pp. 19–22.
[7] D. Naicu, R. A. Harris, and C. Williams, "Timber Gridshells: Design methods and their application to a temporary pavilion," pp. 10–14, Aug. 2014.
[8] F. Khojastehmehr, M. H. Saleh Tabari, and G. H. Filz, "A review on the curvature and geometrical patterns of elastic gridshells: exploring structural and architectural potentials," *Proceedings of the IASS 2022 Symposium affiliated with APCS 2022 conference*, pp. 2573–2586, 2022.
[9] E. Schling and R. Barthel, "Repetitive Structures," in *Gengnagel, Baverel et al. (Ed.) 2020 – Impact: Design With All Senses. DMSB 2019*, pp. 360–375.
[10] P. Block, T. Van Mele, M. Rippmann, and N. Paulson, "Beyond Bending: Reimagining Compression Shells, Edition Detail," 2017.
[11] J. E. Harding, S. Hills, C. Brandt-Olsen, and S. Melville, "The UWE Research Pavilion 2016," in *IASS 2017 Hamburg, Germany*.
[12] G. H. Filz, "Geodesic Winding of Minimal Surfaces: the architecture, structure and geometry of an irregular grid-shell pavilion assembled from thin plywood strips," 2021.
[13] B. D'Amico, A. Kermani, H. Zhang, A. Pungale, S. Colaberlla, and S. Pone, "Timber gridshells: Numerical simulation, design and construction of a full scale structure," *Structures*, vol. 3, pp. 227–235, 2015.
[14] E. Schling, *Inside\Out Gridshell.* [Online]. Available: https://eikeschling.com/2017/11/06/insideout/ (accessed: Jan. 16 2024).
[15] E. Adiels *et al.*, "Design, fabrication and assembly of a geodesic gridshell in a student workshop," 2018.
[16] C. Deregibus and M. Sassone, "Mathematical and structural properties of geodesic curves: an application on a free form gridshell," *Journal of the international association for shell and spatial structures*, vol. 49, 2008.
[17] D. J. Struik, *Lectures on classical differential geometry,* 2nd ed. New York: Dover Publications, 1988, 1961.
[18] E. Adiels *et al.*, "The design, fabrication and assembly of an asymptotic timber gridshell," 2019.
[19] E. Schling, Z. Wan, H. Wang, and P. D'Acunto, "Asymptotic Geodesic Hybrid Timber Gridshell," in *Advances in Architectural Geometry 2023*, K. Dörfler, J. Knippers, A. Menges, S. Parascho, H. Pottmann, and T. Wortmann, Eds.: De Gruyter, 2023, pp. 97–110.

[20] F. Khojastehmehr and G. H. Filz, "Expanding the design freedom of spatial patterns by combined elastic bending and twisting: a parametric study," in *Proceedings of the IASS 2023 Symposium Integrated Design and Fabrication conference*, pp. 28–39.
[21] *An Introduction to Structural Optimization*. Dordrecht: Springer Netherlands, 2008.
[22] Finnish Forest Industries Federation, *Handbook of Finnish Plywood*. Helsinki, Finland: Kirjapaino Markprint Oy, 2007.
[23] D. Piker, *Kangaroo3D.* [Online]. Available: http://kangaroo3d.com/ (accessed: Nov. 21 2023).
[24] Cambridge Dictionary, *Twist.* [Online]. Available: https://dictionary.cambridge.org/dictionary/english/twist (accessed: Dec. 30 2023).
[25] Cambridge Dictionary, *Torque.* [Online]. Available: https://dictionary.cambridge.org/dictionary/english/torque (accessed: Dec. 30 2023).
[26] Merriam Webster Dictionary, *Torque.* [Online]. Available: https://www.merriam-webster.com/dictionary/torque (accessed: Dec. 30 2023).
[27] S. Elmas, G. H. Filz, A. A. Markou, and J. Romanoff, "Zero Gravity: a novel cantilever beam utilizing elastic torsion for structures and architecture," 2021.
[28] R. Naboni, A. Kunic, D. Marino, and H. Hajikarimian, "Robotic zip-bending of wood structures with programmable curvature," *Architecture, Structures and Construction*, vol. 2, pp. 63–82, 2022.
[29] M. H. Saleh Tabari and G. H. Filz, "Cognitive multi-pattern gridshell design: a method inspired by weaverbirds' nest building strategies," in *Proceedings of the IASS Annual Symposium 2023*.
[30] K. Steemers, *DAYLIGHT & ARCHITECTURE: ARCHITECTURE FOR WELL-BEING AND HEALTH.* [Online]. Available: https://www.daylightandarchitecture.com/architecture-for-well-being-and-health/ (accessed: Jan. 26 2024).